Dual Network Effects in the EV Transition: Rise of Charging, Decline of Gas Stations

Yu Hao* Hyuk-soo Kwon† Jinge Li‡

April 29, 2026

Abstract

The transition from internal combustion engine vehicles (ICEs) to electric vehicles (EVs) is shaped by dual network effects: positive feedback between EV adoption and charging-station deployment, and opposing feedback between ICE ownership and gas-station viability. We develop a theoretical and empirical framework in which the two networks co-evolve and compete, generating tipping dynamics in which a market converges to an EV- or ICE-dominated equilibrium according to whether adoption crosses a critical threshold. Using city-level data from China, 2015–2024, we estimate a structural model with random-coefficient demand, dynamic charging-station entry, and Bertrand-Nash pricing on the supply side. Estimated tipping thresholds vary widely across cities and are linked through cross-market spillovers from national pricing, product variety, and battery-cost learning. Counterfactuals show that uniform subsidies are dominated by spatially targeted policies that prioritize low-threshold markets, lowering the cumulative subsidy needed to ignite a self-sustaining transition and informing the optimal timing of policy withdrawal.

Keywords: Electric vehicle, charging station, gas station, network effect, optimal subsidy
JEL Classification: L5, L52, L62, Q58

* University of Hong Kong (haoyu@hku.hk); † University of Chicago (hskwon@uchicago.edu); ‡ Yale University (jinge.li@yale.edu). We would like to thank seminar participants at www, xxx, and conference participants at yyy, zzz for helpful comments.

1 Introduction

The global transition from internal combustion engine vehicles (ICEs) to electric vehicles (EVs) is fundamentally reshaping the transportation industry. A central feature of this transition is the strong interdependence between vehicle adoption and fueling infrastructure. A large literature has documented the complementarity between EV adoption and charging infrastructure: greater availability of charging stations (CSs) increases the attractiveness of EVs, while higher EV adoption raises the profitability of charging investment (e.g., Li et al. (2017); Springel (2021)). However, much less attention has been paid to the parallel—and opposing—dynamics governing gasoline vehicles and gasoline stations (GSs). As EV adoption accelerates, declining demand for ICEs reduces the viability of gasoline stations, leading to exit or underinvestment. This, in turn, further discourages ICE ownership.

This paper studies these dual network effects—the positive feedback between EVs and charging stations, and the competing feedback between ICEs and gasoline infrastructure—and their implications for market dynamics and policy design. We develop a theoretical and empirical framework in which EV–charging and gasoline vehicle–gas station systems evolve jointly and compete for market dominance. When these feedback effects are sufficiently strong, the market exhibits tipping dynamics: below a critical threshold, the economy converges to an ICE-dominated equilibrium, while above it, the EV–charging network becomes self-sustaining and gasoline infrastructure declines. Understanding these tipping dynamics is central not only for characterizing market evolution, but also for policy design: it determines how aggressively policy must act to initiate the transition, and when policy support can be scaled back or withdrawn without reversing it.

These dynamics are not only theoretically relevant but empirically salient in the context of China, the world's largest EV market. EVs accounted for over half of new vehicle sales in 2024, and their share is projected to continue rising. At the same time, the gasoline retail sector—dominated by large state-owned firms—has begun to contract, with evidence of station exit and conversion to charging facilities in EV-intensive regions. As EV adoption expands and ICE sales decline below half of new vehicle sales, the profitability of gasoline stations falls, leading to exit and, in some cases, conversion into charging facilities. This simultaneous expansion of charging infrastructure and contraction of gasoline networks highlights the importance of studying both sides of the transition.

Policy has heavily shaped these developments. China's rapid EV–CS expansion drew

on a broad policy package: the central government provided purchase subsidies of up to 60,000 RMB per vehicle in the early 2010s, declining to 20,000–50,000 RMB through the late 2010s, alongside local matching subsidies that could reach 50 percent of the central amount. EV adoption was further supported through purchase-tax exemptions, and charging infrastructure through construction subsidies and per-kWh usage subsidies of roughly 0.1–0.2 RMB in many cities. Beginning in 2019, local governments were encouraged to shift away from upfront purchase subsidies toward infrastructure and usage-based support, reinforcing charging network expansion.

These policies have since been phased out or restructured. Central subsidies were sharply reduced starting in 2019 and eliminated at end-2022, while tax exemptions are scheduled to remain through 2027. Despite the removal of large purchase subsidies, EV adoption has continued to accelerate, fueling speculation that the EV–CS system has entered a self-sustaining regime sustainable by market forces alone. A large literature studies how to initiate an EV transition; far less attention has been paid to how and when policy support can be optimally withdrawn. We argue that the answer depends fundamentally on the strength of dual network effects and the shape of tipping dynamics.

An important implication of our framework is that tipping dynamics are inherently heterogeneous across markets and interconnected across space. The location of the tipping point depends on local conditions, including consumer preferences, population density, infrastructure costs, and geographic constraints, implying that some markets are naturally more "EV-friendly" than others. At the same time, markets are not independent. Automakers make product portfolio and pricing decisions at the national level, and upstream technological progress—such as learning-by-doing in battery production (Barwick et al. (2025))—links EV adoption across regions. As a result, EV-CS network expansion in one market can generate positive spillovers to others, effectively lowering their tipping thresholds over time.

These considerations suggest optimal policy is unlikely to take the form of uniform subsidies. A more efficient strategy concentrates early support in low-tipping-point markets, where the EV–CS network reaches self-sustainability fastest, and lets cross-market spillovers carry adoption to higher-threshold markets. This pattern matches the policy record: China piloted EV promotion in a small set of cities before nationwide rollout, and U.S. adoption has been driven disproportionately by California and a few other states.

Accounting for cross-market spillovers and heterogeneous tipping points is essential for both the timing of policy withdrawal and the spatial allocation of policy effort during the transition.

We first introduce a stylized theoretical framework to characterize tipping dynamics between two stable steady states—EV–CS–dominated and ICE–GS–dominated equilibria—and to identify the key forces that determine the location of tipping points. To identify the tipping thresholds of Chinese cities, we develop a structural model that captures both the complementary between EVs and charging stations and the competing network effects between ICE vehicles and gasoline infrastructure. In the model, consumers choose vehicles based on prices, product attributes, and the availability of charging or refueling infrastructure; charging and gasoline station operators make dynamic entry and exit decisions in response to local market conditions, including geographic characteristics and the evolution of EV and ICE stocks; and automakers set prices and product portfolios to maximize static profits at the national level.

Our demand estimation builds on the discrete choice framework of Berry et al. (1995), which accommodates flexible substitution patterns and addresses price endogeneity using instrumental variables. In addition, to tackle the endogeneity of charging infrastructure, we construct Bartik-style instruments, following a well-established approach in urban and labor economics (Bartik, 1991; Goldsmith-Pinkham et al., 2020). On the supply side, we model charging station entry as a dynamic discrete choice problem within the class of dynamic structural models pioneered by Rust (1987) and extended to strategic settings by Ericson and Pakes (1995). Estimation proceeds via a two-step approach in the spirit of Hotz and Miller (1993) and Aguirregabiria and Mira (2007), which alleviates the computational burden associated with solving the full dynamic game.

We use the estimated model to characterize tipping points and inform optimal policy design. The tipping threshold depends both on the relative attractiveness of EVs compared to ICE vehicles and on the strength of infrastructure network effects. These forces vary across markets with differences in consumer preferences, population density, and infrastructure costs. Moreover, adoption in one market can spill over to others through firms' national pricing and product portfolio decisions: greater EV variety and intensified competition that lowers prices can reduce tipping thresholds economy-wide. These features imply that uniform policy interventions may be inefficient. Instead, targeting markets with

low tipping thresholds—where policy can more readily make the EV–CS network self-sustaining—can generate spillovers that accelerate adoption elsewhere. Building on this insight, we examine the optimal allocation of EV subsidies across markets over time.

This paper contributes to three strands of the literature. First, it contributes to a broad literature on policies designed to accelerate the adoption of new technologies, such as clean vehicles (Aghion et al. (2016); Holland et al. (2021); Kwon (2026)), clean energy (Feger et al. (2022); Dorsey (2024)), as well as general green technologies (Acemoglu et al. (2012, 2016); Aghion et al. (2025); Dugoua and Moscona (2025)). Existing work shows that policy interventions affect the transition to new technologies through consumer adoption incentives, firms' innovation incentives, market structure, and competition intensity, jointly shaping both the pace and equilibrium outcomes of the transition toward cleaner technologies. Our paper complements this line of work by studying not only how policies facilitate the transition, but also when such policies can be optimally withdrawn, with particular emphasis on the end of transition policies. A few studies examine how the phase-out of policies (Hu et al. (2025); De Groote and Verboven (2019); Lohawala (2023)), affects consumer demand and firms' strategic responses. Our paper differs by explicitly characterizing the safe timing of policy exit that ensures the new technology becomes self-sustaining.

Second, this paper contributes to a growing literature on complementarities across clean technologies and the network effects they generate—between EVs and charging infrastructure (Li et al. (2017); Meunier and Ponssard (2020); Springel (2021); Li (2023); Remmy (2025); Barwick et al. (2026)), EVs and solar panels (Garcia-Osipenko (2025)), solar and battery storage (Bollinger et al. (2024); Butters et al. (2025)), battery technology and EVs (Barwick et al. (2025)), and EVs and high-speed rail (Fang et al. (2025)). These papers document how positive feedback shapes diffusion and how policies targeting one technology spill over to its complements. We extend this work beyond a single complementary network to a setting with competing networks. Competing dual network effects generate unstable tipping dynamics, in which small policy differences lead to large shifts between technologies. Accounting for these cross-network interactions changes optimal policy design materially.

Finally, this paper contributes to a vast literature on network effects and tipping dynamics. A large body of theory work shows how network externalities shape multiple equilibria and equilibrium selection, generating path dependence or incumbency advantages. (Katz

and Shapiro (1985, 1986); Farrell and Saloner (1986); Ellison et al. (2003); Rochet and Tirole (2003); Armstrong (2006)). Complementing this, empirical studies quantify network effects across settings such as software, payment systems, telecommunications, and platform competition (Gandal, 1994, 1995; Ackerberg and Gowrisankaran, 2006; Björkegren, 2019, 2022; Brown and Morgan, 2009; Cao et al., 2021), documenting that while network effects can lead to dominance, coexistence often arises due to heterogeneity and frictions. Our paper builds on this literature but extends it by studying a setting in which multiple markets are interconnected through spillovers from firms' national pricing, product portfolios, and technological progress. This interdependence implies that optimal policy must account for both within-market tipping and across-market spillovers, guiding the sequencing and spatial targeting of interventions across markets.

2 Theoretical Framework

This section develops a stylized framework to study the transition of EVs and the corresponding evolution of infrastructure with the presence of two-sided network effects. It shows that sufficiently strong network effects generate tipping dynamics, characterized by multiple steady states and a critical adoption threshold. Below the threshold, the market converges to a low-EV equilibrium dominated by gasoline vehicles and gasoline stations. Once adoption exceeds the tipping point, feedback between vehicle purchases and infrastructure expansion drives the economy toward a high-EV equilibrium, even in the absence of further policy intervention.

2.1 Setup

Time is discrete and indexed by t. The economy consists of consumers choosing between EVs and ICEs, and firms operating CSs and GSs. $e_t \in [0,1]$ denotes the share of EVs in the vehicle stock at time t. Consumers choose between EVs and ICEs based on their preferences and the availability of fueling infrastructure. Let $x_t \in [0,1]$ denote the density of CSs, while $y_t \in [0,1]$ represents the density of GSs. CSs and GSs enter and exit in response to vehicle shares. Let infrastructure evolve according to

$$x_{t+1} = (1-\rho_x)x_t + \rho_x G_x(e_t), \tag{1}$$

$$y_{t+1} = (1-\rho_y)y_t + \rho_y G_y(1-e_t), \tag{2}$$

where $\rho_x, \rho_y \in (0,1)$ capture adjustment speeds (e.g., due to entry and exit costs). The functions $G_x(\cdot)$ and $G_y(\cdot)$ represent the required infrastructure levels in the current period and correspond to the long-run station densities implied by free entry. They satisfy

$$G_x(0) = G_y(0) = 0, \quad G_x(1) = G_y(1) = 1 \tag{3}$$

$G_x(0) = G_y(0) = 0$ implies that when there are no vehicles of a given fuel type, no corresponding infrastructure is provided. In contrast, $G_x(1) = G_y(1) = 1$ indicate that when a single fuel type fully dominates the vehicle stock, the associated infrastructure reaches its normalized saturation level.

The utility difference between EVs and ICEs includes, in addition to consumer-specific

preferences θ_{0i} for EVs over ICEs,

$$\Delta U_t = \theta_0 + H_x(x_t) - H_y(y_t), \tag{4}$$

where θ_0 captures the intrinsic relative attractiveness of EVs (e.g., operating cost, performance, and autonomous driving). The increasing functions $H_x(\cdot)$ and $H_y(\cdot)$ measure consumers' evaluations of infrastructure. The EV stock share adjusts according to

$$e_{t+1} = (1-\rho_e)e_t + \rho_e F(\Delta U_t), \tag{5}$$

where ρ_e captures the speed of adjustment in vehicle ownership (e.g., the frequency of new car purchases and vehicle scrappage rates). F is an increasing function of ΔU_t and satisfies

$$F(\theta_0 + H_x(0) - H_y(y_t)) = 0, \quad F(\theta_0 + H_x(x_t) - H_y(0)) = 1 \tag{6}$$

The first condition means that when no CSs are available, no consumers choose EVs. The second condition indicates that when no GSs are available, no consumers choose ICEs.

2.2 Steady States

In a steady state, we have

$$x = G_x(e), \quad y = G_y(1-e), \quad e = F(\theta_0 + H_x(x) - H_y(y)). \tag{7}$$

Define a mapping T, which determines the long-run behavior of the industry dynamics:

$$T(e) \equiv F\left(\theta_0 + H_x(G_x(e)) - H_y(G_y(1-e))\right). \tag{8}$$

Then, steady states satisfy $T(e) = e$. By construction, there exist at least two steady states:

$$T(0) = F\left(\theta_0 + H_x(0) - H_y(1)\right) = 0, \quad T(1) = F\left(\theta_0 + H_x(1) - H_y(0)\right) = 1 \tag{9}$$

$e = 0$ represents the no-EV state, while $e = 1$ corresponds to the all-EV state. The natural questions are whether there are additional steady states between these two and what conditions give rise to them.

2.3 Assumptions and Chicken-and-Egg Problem

First, we assume H_x and H_y are strictly increasing and continuously differentiable. Thus, consumer utility gradually increases with infrastructure until it is saturated at $x = 1$ or $y = 1$. Second, F is strictly increasing and continuously differentiable. This requires that consumer preferences θ_{0i} for EVs relative to ICEs are heterogeneous and continuously distributed across the population. By contrast, if preferences were homogeneous, F would collapse to a binary (0–1) function. Lastly, G_x and G_y are strictly increasing and continuously differentiable. Economically, this implies heterogeneity in location suitability and firm cost structures for infrastructure provision. Some locations are more attractive for CS or GS entry (for example, due to higher traffic or demand density), while others are more isolated and cannot support entry unless the EV or ICE share is sufficiently large. In addition, differences in firms' cost structures can generate a smooth aggregate entry response.

Second, we impose assumptions on the slopes of the functions at the endpoints ($e = 0$ and $e = 1$). Differentiating $T(e)$ yields a positive, continuous function:

$$T'(e) = \tag{10}$$
$$F'\big(\theta_0 + H_x(G_x(e)) - H_y(G_y(1-e))\big)\left[H_x'(G_x(e))G_x'(e) + H_y'(G_y(1-e))G_y'(1-e)\right] > 0.$$

We introduce the classic chicken-and-egg problem with the following assumptions:

$$T'(0) = F'\big(\theta_0 + H_x(0) - H_y(1)\big)\left[H_x'(0)G_x'(0) + H_y'(1)G_y'(1)\right] < 1, \tag{11}$$
$$T'(1) = F'\big(\theta_0 + H_x(1) - H_y(0)\big)\left[H_x'(1)G_x'(1) + H_y'(0)G_y'(0)\right] < 1. \tag{12}$$

These conditions ensure that both the no-EV state and the all-EV state are locally stable. In particular, $T'(0) < 1$ implies that the no-EV state is stable: when only a very small number of consumers adopt EVs and CS are extremely scarce, this situation cannot be sustained. Low EV adoption leads to CS exit (e.g., $G_x'(0)$ is small), and limited CS availability discourages EV purchases (e.g., $F'(\theta_0 + H_x(0) - H_y(1))$ is small). Similarly, $T'(1) < 1$ implies that the all-EV state is stable: when only a small number of ICEs and GSs remain, this configuration is not sustainable. Consumer demand for ICEs is too low to support profitable GS operation (e.g., $G_y'(0)$ is small), and GS are too sparse to make ICE ownership attractive (e.g., $F'(\theta_0 + +H_x(1) - H_y(0))$ is small).

Figure 1: Tipping Point and Steady States

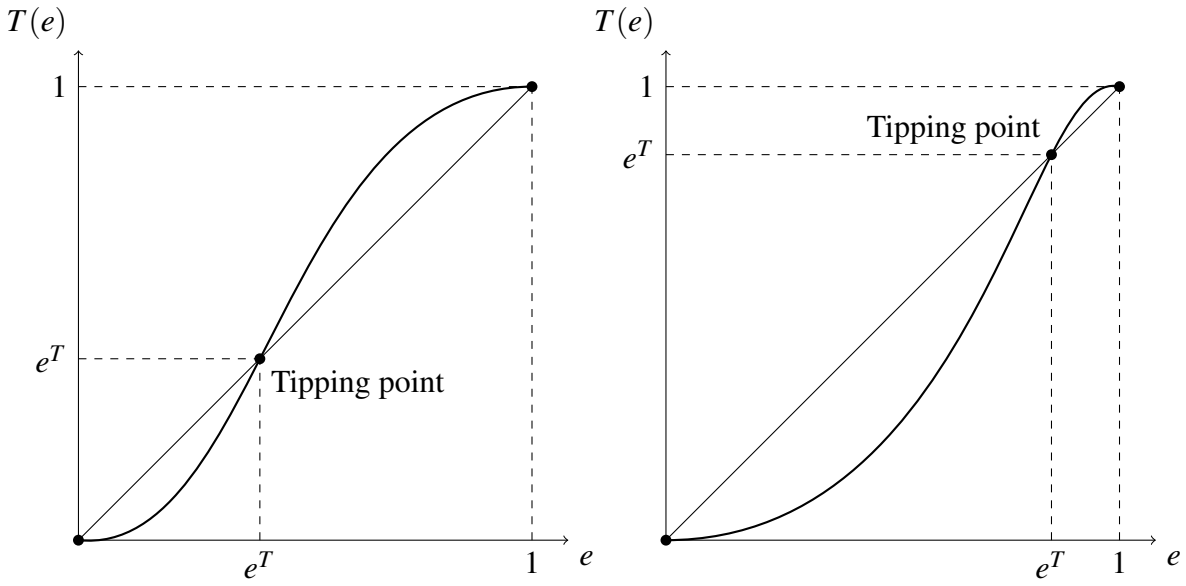

(a) Easy-to-Sustain EV Technology

(b) Hard-to-Sustain EV Technology

2.4 Tipping Point

With the chicken-and-egg assumptions, there is at least one interior steady state between the no-EV and all-EV states, as shown in Figure 1. Unlike the two endpoints, this interior steady state is unstable and serves as a tipping threshold. If e exceeds e^T, the EV–CS network expands while the ICE–GS network contracts, and the system converges to the all-EV state. If e falls below e^T, the reverse dual network effects work and the industry converges to the no-EV state. The key question is where this tipping point is located. The tipping point in Panel (a) is lower than in Panel (b), indicating that EV adoption is more easily self-sustaining in the former case than in latter case. Two factors affect the tipping point location.

Intrinsic Advantage of EV Technology First, it depends on the intrinsic relative attractiveness of EV technology, represented by θ_0 in this model. Many factors influence θ_0. For example, advances in autonomous driving, declines in battery costs that reduce EV prices, and fast-charging technology improving charging convenience raise θ_0. A higher θ_0 shifts $T(\cdot)$ upward and lowers the tipping point, making EV technology more self-sustaining.

Dual Network Effect Second, the location of the tipping point depends on the strength of the dual network effects between vehicles and infrastructure. The slope of $T(\cdot)$ depends on

$$H_x'(G_x(e))G_x'(e) + H_y'(G_y(1-e))G_y'(1-e), \tag{13}$$

where $H_x' > 0$ and $G_x' > 0$ measure the CS-to-EV and EV–to-CS network effects, while $H_y' > 0$ and $G_y' > 0$ measure the GS-to-ICE and ICE–to-GS network effects. Together, these terms summarize the total dual network feedback. When these network effects are strong during the early EV adoption period, it shifts $T(\cdot)$ upward and lowers the tipping point, accelerating the transition toward the EV-dominant equilibrium.

2.5 Policy Implications

- The actual evolution of vehicle stock and infrastructure is subject to adjustment frictions and depends on δ_s (purchase frequency and scrappage rates), δ_x, and δ_y (CS and GS entry and exit frictions). With greater frictions (i.e., small δ parameters), transitions from one steady state to another take longer.
- Once the economy passes the unstable steady state, government support is no longer necessary to sustain EV adoption. Thus, the tipping point is the policy goal line. The sufficient conditions to pass the long-run tipping point are:

$$e_t > e^T, \quad H_x(x_t) - H_y(y_t) > H_x(G_x(e^T)) - H_y(G_y(1-e^T)). \tag{14}$$

- If the tipping point is very high, continuous government support for the EV industry is necessary, since EV adoption would otherwise gradually dissipate before reaching the threshold.
- The location of the tipping point is fundamentally an empirical question, determined by consumer preferences and infrastructure costs. We therefore need to estimate flexible functional forms for the $H(\cdot)$ and $G(\cdot)$ functions to convince readers.
- Suppose markets differ in their tipping thresholds due to heterogeneity in consumer preferences, infrastructure costs, population density, and geographic conditions. Suppose further that markets are linked through spillovers, such as national pricing and model entry decisions by automakers and endogenous technological progress (e.g., battery cost

reductions).

[Conjecture] *In this environment, concentrating early EV promotion in low-tipping markets and expanding gradually to high-tipping markets may be a more efficient (less costly) approach than uniform promotion across all markets.*

EV–CS networks are more likely to become self-sustaining in these low-tipping markets after sufficiently long government support. These self-sustaining markets can then generate positive spillovers to high-tipping markets, lowering their effective tipping points over time.

2.6 (Optional) Tipping Range

In theory, multiple tipping points can arise, as illustrated in Figure 2. In this case there are two unstable steady states, e^{T1} and e^{T2}. If the EV share falls between these two thresholds, EV and ICE technologies can coexist without government intervention; we refer to this interval as the tipping range. Once the long-run EV share exceeds e^{T1}, the EV–CS network becomes self-sustaining without policy support. In addition, once it exceeds e^{T2}, the ICE–GS network begins to phase out gradually without additional intervention.

Figure 2: Multiple Tipping Points and Tipping Range

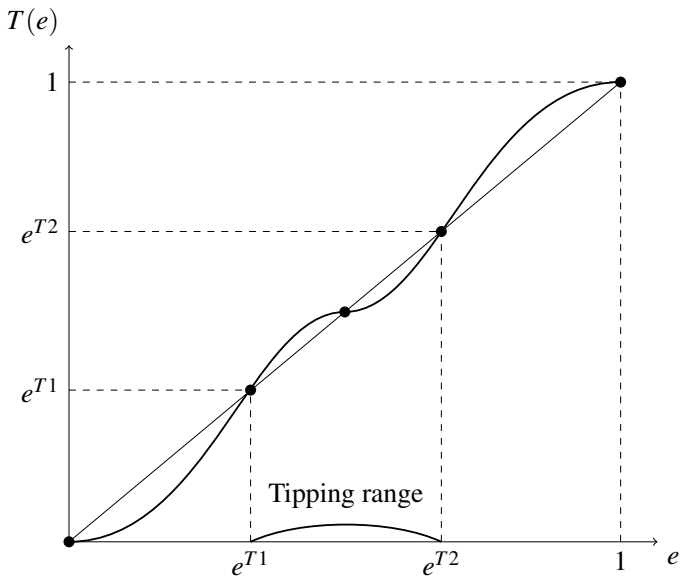

3 Industry Background and Policy

3.1 Policy

China began promoting new energy vehicles (NEVs) in 2009, and the market has since experienced explosive growth. By 2022, annual passenger NEV sales in China had surpassed several million units, accounting for over 60% of global EV sales and making China the world's largest EV market. This rapid market expansion was driven in large part by generous consumer purchase subsidies from both central and local governments, as well as a range of non-financial incentive policies.

Central EV purchase subsidies. The central government's consumer purchase subsidies were initially implemented in select pilot cities before 2014, then expanded nationwide in 2016. Consumers pay the post-subsidy price at the time of purchase, and subsidies are distributed to automakers by the government. Subsidies for battery electric vehicles (BEVs) are notched based on electric driving range cutoffs, while plug-in hybrid electric vehicles (PHEVs) receive a uniform subsidy with a minimum range requirement of 50 km. From 2015 to 2022, central subsidies underwent a continuous phase-down: for the highest-range BEVs, subsidies declined from over 50,000 RMB in 2015 to 12,600 RMB in 2022, before being fully phased out at end-2022; PHEV subsidies fell from 31,500 to 4,800 RMB over the same period. Concurrent with the subsidy reduction, eligibility thresholds were progressively tightened, steering the industry toward longer range, higher energy density, and greater energy efficiency. Figure 3 Panel A presents the evolution of subsidy amounts by BEV range tier and for PHEVs. We code the subsidy rules for each year from official policy documents and combine them with vehicle-specific technical parameters to compute the central subsidy for each vehicle model; Appendix A provides the full construction details.

Local EV purchase subsidies. In addition to the central subsidies, many cities provided supplementary local consumer purchase subsidies that exhibited substantial cross-city heterogeneity. Most cities set local subsidies as a proportion of the central subsidy—typically ranging from 20% to 100%—while some cities adopted fixed-amount schedules. Similar to central subsidies, local subsidies experienced annual phase-downs and were largely phased

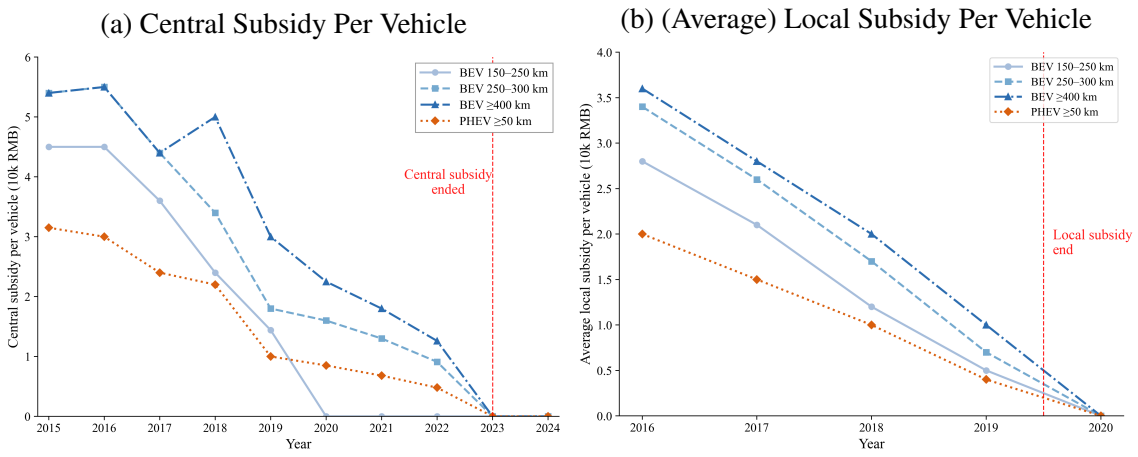

Figure 3: National EV purchase subsidy schedule, 2015–2023. Panel A: Central government subsidy per vehicle (10,000 RMB) by BEV range tier and PHEV. Amounts are base subsidies before battery density and energy efficiency adjustments. Subsidies were fully phased out at end-2022. Panel B: Average local government subsidy per vehicle (10,000 RMB). Subsidies were largely phased out by mid-2019.

out by mid-2019. Figure 3 Panel B shows the average local subsidy per vehicle over time. We systematically compiled local subsidy policies across sample markets from the PKU-LAW legal database and computed vehicle-specific local subsidies; see Appendix A for details.

Charging station subsidies. To accelerate charging infrastructure deployment, both central and local governments offered construction subsidies (RMB/kW installed) and usage subsidies (RMB/kWh dispensed). Figure 4 Panel A traces the national guideline for construction subsidies alongside city-level effective rates. The national guideline declined from 600 RMB/kW (2016) to zero, but cities exhibited substantial heterogeneity: for example, Beijing raised its effective rate to 1,000 RMB/kW in 2024 even as the national benchmark fell. Panel B shows usage subsidies, which typically range from 0.1 to 0.4 RMB/kWh and exhibit less temporal variation. This city-level heterogeneity in charging subsidies provides cross-sectional variation that we exploit in the entry model. Early entrants benefited from substantial construction grants and steady usage subsidies, while later entrants faced a much thinner subsidy envelope—a temporal gradient that our entry model captures through the time-varying subsidy state variables σ_{ct}^{bld} and σ_{ct}^{use}. Appendix A provides a detailed quantification of these subsidies.

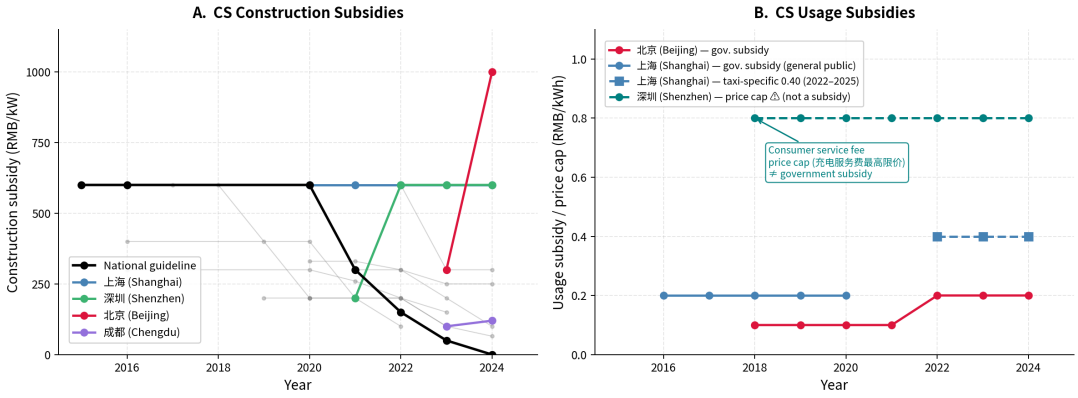

Figure 4: Charging station subsidies, 2015–2024. Panel A: Construction subsidy (RMB/kW) — national guideline (black) vs. city-specific effective rates (colored lines: Beijing, Shanghai, Shenzhen, Chengdu; gray lines: other cities). Panel B: Usage subsidy (RMB/kWh dispensed) for cities with positive usage subsidies. Data from 1,261 PKULAW policy documents, constructed in `subsidy_panel.csv`.

3.2 Data

Vehicle Sales We construct a product-level panel of new vehicle sales across Chinese cities from 2015 to 2024. The raw data cover the universe of new passenger vehicle registrations from China's vehicle registration database, with each record identifying the vehicle's registration district, month, manufacturer, brand, model, fuel type, body type, and transaction price. We aggregate district-month records to the city-year-model level. Each product j in market m (city $\times$ year) is defined by the unique combination of manufacturer, brand, model, fuel type, body type, and size segment.

Vehicles are classified into five fuel types: ICEV (gasoline, diesel, methanol, and fuel cell), BEV (battery electric), PHEV (plug-in hybrid), REEV (range-extended electric), and HEV (hybrid electric). We define "electric vehicles" (EV) as the union of BEV, PHEV, and REEV — the three categories eligible for new energy vehicle (NEV) subsidies and license plate preferences. Product characteristics include MSRP, maximum power, displacement, exterior dimensions, fuel efficiency, electric driving range, electric motor power, battery capacity, and electric efficiency. Missing characteristics are imputed using a two-stage procedure described in Appendix C.

Infrastructure Data We construct market-level counts of public charging stations ($N_{\text{cs},m}$) and gas stations ($N_{\text{gs},m}$) using fitted measures that interpolate across administrative bound-

Table 1: Summary Statistics

	GVs			EVs		
	# of Obs.	Mean	Std. Dev.	# of Obs.	Mean	Std. Dev.
Panel A: Model-year-city observations for demand-side analysis						
Quantity	378,766	502.01	1,269.91	118,097	260.20	1,099.28
Price (10k RMB)	378,766	15.64	12.05	118,097	20.31	13.31
Fuel efficiency (L/100km)	378,766	6.96	1.29	118,097	0.44	0.76
Electric efficiency (kWh/100km)	–	–	–	118,097	14.95	3.82
Horsepower (log)	378,766	4.71	0.30	118,097	4.62	0.61
EV range (log km)	–	–	–	118,097	5.54	0.79
Central subsidy (10k RMB)	–	–	–	118,097	0.70	1.25
Duration	378,766	3.70	2.37	118,097	2.76	1.85

Notes: Panel A shows the summary statistics for the data used for the demand estimation, with the unit of observation being city by year by model in the 52 cities plus 27 province residuals during the sample period (2015–2024).

	# of Obs.	Mean	Std. Dev.	Min	Max
Panel B: Infrastructure					
# of Charging Stations	790	632.56	893.89	0	6,668
# of Gas Stations	790	1,334.20	1,599.38	85	10,714
Panel C: Market Structure					
# of Manufacturers	790	78.91	7.67	57	103
# of BEV Models	790	105.03	83.49	0	313
# of PHEV Models	790	38.03	32.65	0	116
# of ICEV Models	790	454.15	65.81	227	595
# of HEV Models	790	25.30	17.87	3	60
# of REEV Models	790	6.42	10.13	0	36

Notes: Panel B reports the number of hexagons containing charging stations and gas stations across market observations (we use hexagons as proxies for stations). Panel C reports the number of manufacturers and vehicle models by type in each market.

aries to align with our definition of c. Both variables enter the demand model in logarithmic form, $\log(N_{\text{cs},m})$ and $\log(N_{\text{gs},m})$.

For the entry model, we use spatially disaggregated charging station locations mapped to H3 hexagonal grid cells at resolution 9 (approximately 0.105 km^2 per cell). We retain hexagons classified as built-up area and classify each into three tiers — thriving,

commercial, and remote — based on pre-sample (2014) points-of-interest density, which serves as a time-invariant geographic characteristic free of simultaneity concerns. We define the feasible region as the union of thriving and commercial hexagons, and construct the entry panel at the city $\times$ year $\times$ tier level, yielding tier-specific entry densities $d_{\tau,ct} = D_{\tau,ct}/N_{\tau,c}$ (stations per hex). City-year gas station counts are compiled from industry databases and enter the tipping model via the calibrated exit equation. Further details on the spatial classification and data cleaning procedures are provided in Appendix C.

3.3 Descriptive Patterns

Charging stations and EV adoption. Figure 5 presents the geographic distribution of charging stations and EV stock shares across Chinese provinces in 2015, 2020, and 2024. In 2015, charging infrastructure was minimal and highly concentrated in a few eastern provinces (Beijing, Shanghai, and Guangdong). By 2024, all provinces had developed extensive charging networks, with the highest counts exceeding 6,000 stations in provinces such as Guangdong and Zhejiang. The share of EV stocks (bottom row) follows a similar diffusion pattern, increasing from near-zero levels in 2015 to 5–18% by 2024, with coastal and southern provinces leading the adoption. This spatial pattern is consistent with a strong correlation between charging infrastructure and EV adoption, motivating our subsequent analysis of infrastructure-driven network effects.

Gas stations and the gasoline fleet. Figure 6 presents the corresponding maps for gas stations and ICE stock shares. The gas station network was already well-established in 2015 and exhibits relatively limited changes by 2024, with the highest densities observed in provinces such as Shandong, Hebei, and Guangdong. The ICE stock share (bottom row) exceeded 99% nationwide in 2015. By 2024, there is substantial spatial variation: ICE shares have declined to below 85% in provinces such as Guangdong and Hainan, while remaining above 95% in most interior regions. The contrast between the relatively stable gas station network and the rapid expansion of charging infrastructure highlights the asymmetric evolution of the two networks, which lies at the core of the dual network effects we study.

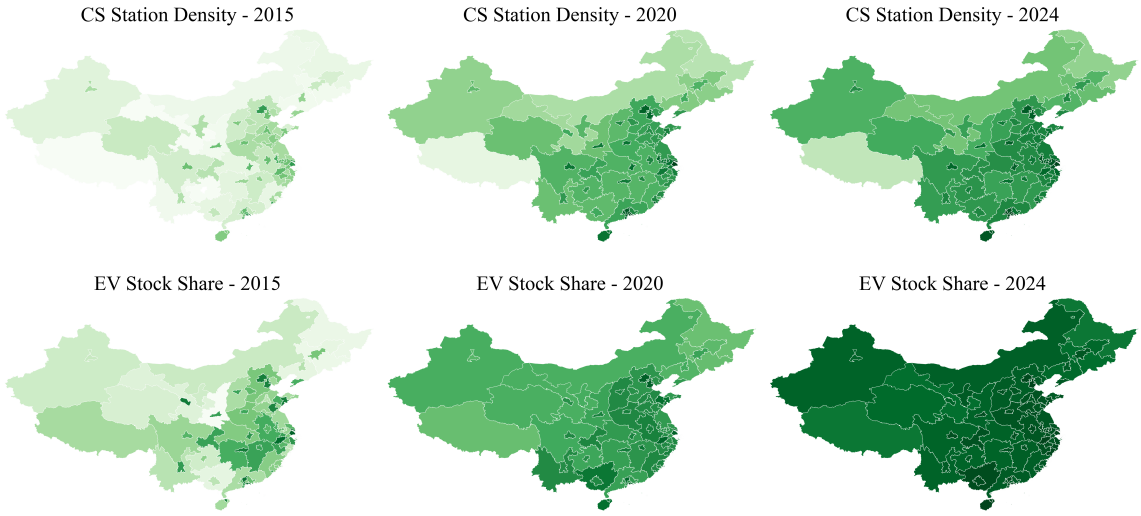

Figure 5: City-level charging station density (top row) and EV stock density (bottom row) for 2015, 2020, and 2024. Both are aggregated to 52 sample cities and 27 provinces residual markets. EV stock share computed via perpetual inventory ($\delta = 0.10$). The co-evolution of infrastructure and adoption across space and time is consistent with positive feedback between the two.

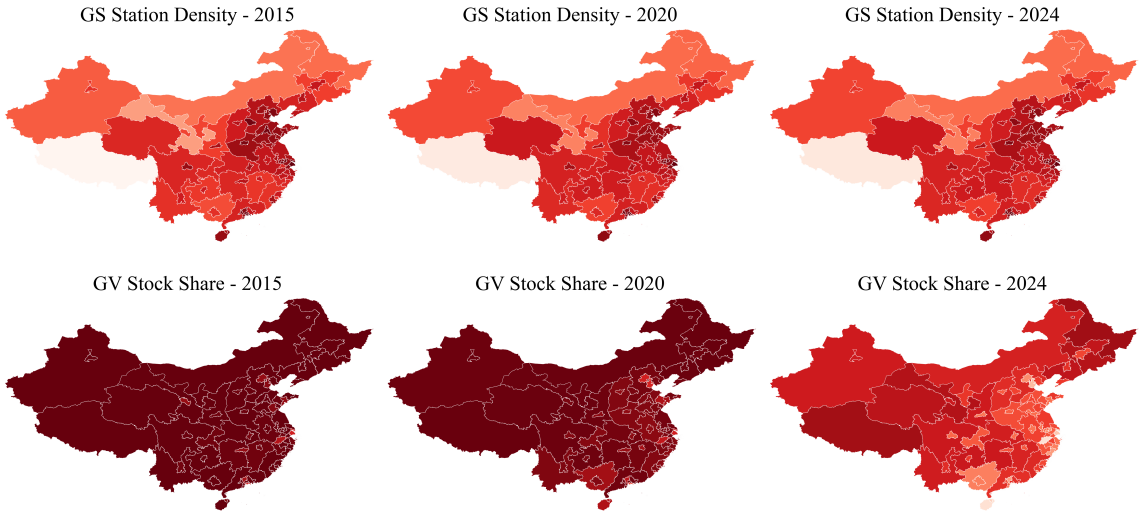

Figure 6: City-level gas station density (top row) and gasoline vehicle stock share (bottom row) for 2015, 2020, and 2024. Gas station counts from the demand estimation sample (79 markets). ICE stock share equals $1 - s_{\text{ev}}$. The gas station network is spatially stable, while ICE dominance erodes heterogeneously across provinces — fastest in coastal and southern regions where EV adoption leads.

Vehicle sales and infrastructure expansion We further examine the correlation between vehicles sales and infrastructure expansion as shown in Figure 7. After partialling out city

(a) Residualized BEV Sales over Residualized CS

(b) Residualized GV Sales over Residualized GS

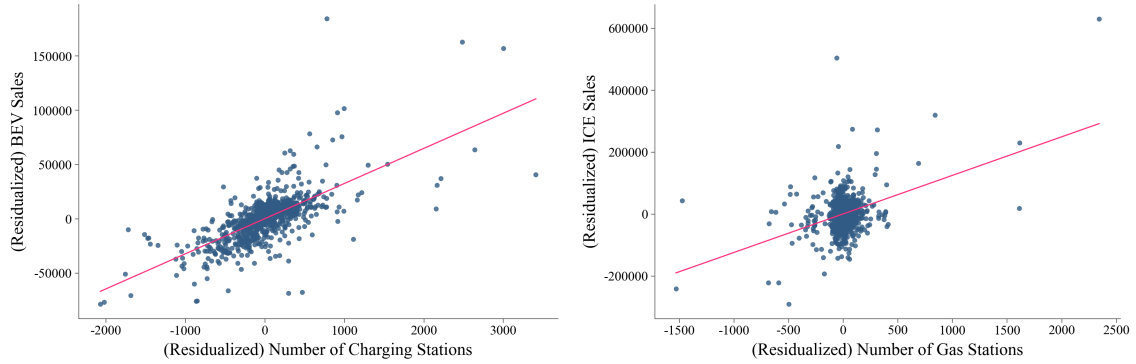

Figure 7: Correlation graph between Vehicle sales and station numbers. It plot residualized BEV (panel a) and ICE (panel b) sales against the residualized number of charging stations and gas stations, respectively. Residuals are obtained after controlling for province and year fixed effects, as well as a set of time-varying controls. Each observation corresponds to a city-year pair. The solid line represents the linear fit.

and year fixed effects, as well as population and GDP per capita, panel 7a illustrates changes in BEV sales residuals over charging station residuals. The blue dots represents the vehicle sales residuals over charging station residuals for each city at each year. The BEV sales and charging stations exhibit a positive correlation. Figure 7b presents the analogous relationship between gas stations and GV sales using residualized variation. The association between gas stations and GV sales appears positive.

3.4 Charging station entry and location prosperity

Figure 8 uses hex-level data (H3 resolution 9, $\approx$0.1 km^2 per cell) to examine the relationship between location quality and charging station entry, where location quality is measured continuously by the total number of nearby points of interest (restaurants and retail stores within 2.5 km). We use three cross-sections (2018, 2021, 2024) covering 52 cities and approximately 3 million hex-year observations and fit a gradient boosting classifier (GBC) to predict the binary entry outcome $\mathbf{1}[\text{CS count} > 0]$ as a function of local POI density, city-level EV stock share, economic characteristics, and subsidy levels.

Panel A presents binscatter plots of entry probability against POI count, stratified by EV stock share terciles. Two patterns stand out. First, entry probability rises steeply with

location prosperity: hexes with 1,000+ POIs are 40–60 percentage points more likely to host a charging station than hexes with zero POIs. Second, higher EV adoption uniformly shifts the curve upward—at every level of location quality, cities with higher EV shares exhibit greater entry.

Panel B shows partial dependence plots (PDPs) from the GBC, fixing EV stock share at 2%, 8%, and 20% while varying POI density. The interaction is pronounced: at low EV adoption ($s_{\text{ev}} = 2\%$), even prime locations have modest entry probability ($\sim$20%); at high adoption ($s_{\text{ev}} = 20\%$), entry probability exceeds 60% for well-located hexes. This non-parametric evidence confirms that infrastructure supply responds to both location fundamentals and the installed EV base.

Panel C compares predicted entry under observed subsidies versus a no-subsidy counterfactual. The subsidy effect is positive but modest—construction and usage subsidies account for roughly 1–3 percentage points of additional entry probability, consistent with the low feature importance of subsidy variables in the GBC (combined $\approx$1.3%). This suggests that location quality and EV adoption, rather than direct subsidies, are the primary drivers of entry.

Panel D shows PDPs of entry probability against EV stock share, stratified by POI terciles. High-POI locations respond most strongly to EV adoption: their entry probability rises from $\sim$20% at $s_{\text{ev}} = 0$ to $\sim$70% at $s_{\text{ev}} = 30\%$. Low-POI locations remain largely unresponsive regardless of EV penetration, confirming that the entry margin operates primarily through commercially viable locations.

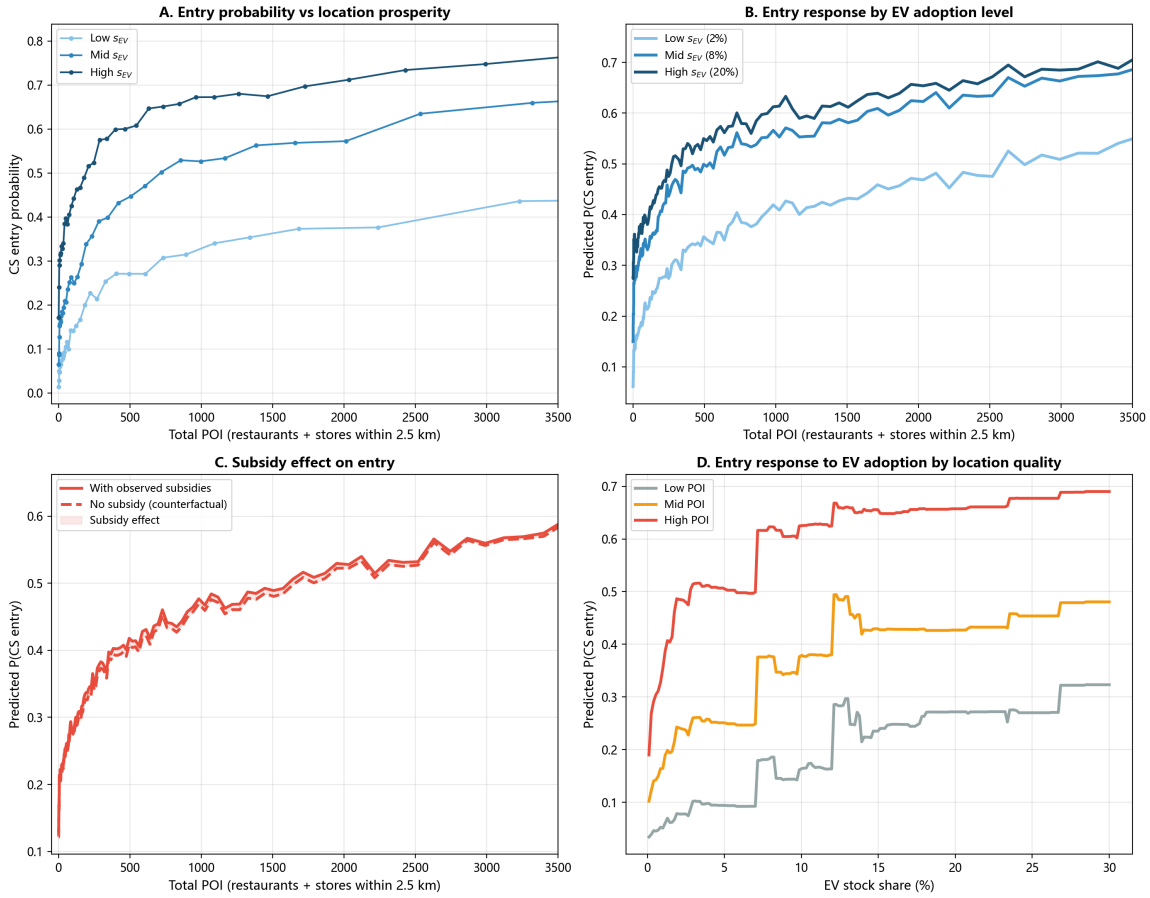

Figure 8: Hex-level charging station entry probability vs. location prosperity. Panel A: Binscatter of entry probability against total POI count (restaurants + stores within 2.5 km), stratified by city-level EV stock share terciles. Panel B: GBC partial dependence of entry probability on POI density at three fixed EV stock share levels (2%, 8%, 20%). Panel C: Predicted entry with observed subsidies (solid) vs. no-subsidy counterfactual (dashed). Panel D: Partial dependence on EV stock share by POI tercile—high-quality locations respond most strongly to EV adoption. Data: H3 res-9 hexes $\times$ {2018, 2021, 2024}, 52 cities, $\approx$2.9M observations. GBC with 500 trees, max depth 5. Feature importances: POI density 52%, s_{ev} 29%, urbanization 7%, pop. density 6%.

4 Demand Estimation

4.1 Model

We model consumer demand using a logit framework at the market level, where each market is defined as a city–year pair. Consumer i chooses from a set of available products $J = \{0, 1, 2, \ldots, J\}$ that includes both ICEs and EVs, where $j = 0$ represents the outside option of not purchasing a new vehicle. Consumer i's utility from vehicle model j ($j \neq 0$) in market m is specified as:

$$u_{ijm} = \alpha \log p_{jm} + \beta_{\text{gs}} \mathbf{1}_{\text{ICE}} \cdot f(N_{\text{gs},m}) + \beta_{\text{cs}} \mathbf{1}_{\text{EV}} \cdot f(N_{\text{cs},m}) + X_{jm}\gamma + \xi_{jm} + \varepsilon_{ijm}. \quad (15)$$

The utility of the outside option is normalized to zero where $u_{ijm} = 0$ for all i,and m. p_{jm} is the transaction price defined in Equation 26 that accounts for subsidy and tax. $N_{\text{gs},m}$ and $N_{\text{cs},m}$ denote the number of gas stations and charging stations in market m, respectively, and infrastructure enters the utility function through a flexible transformation $f(\cdot)$, interacted with fuel-type indicators. X_{jm} consists of two components. The first is a vector of vehicle characteristics, including vehicle size, engine power, driving range for EVs, and fuel-type-specific energy consumption. The second is a rich set of fixed effects, including brand, fuel type, body type, city and year fixed effects, and duration fixed effects. The duration variable measures the number of periods since a model first enters the market. ξ_{jm} represents unobserved attributes of model j or demand shocks to j in market m, and ε_{ijm} is an idiosyncratic preference shock which is assumed to have an i.i.d. Type-I extreme value distribution.

Under the standard logit assumption, aggregation yields the linear estimating equation:

$$\log(s_{jm}/s_{0m}) = \alpha \log p_{jm} + \beta_{\text{gs}} \mathbf{1}_{\text{ICE}} \cdot f(N_{\text{gs},m}) + \beta_{\text{cs}} \mathbf{1}_{\text{EV}} \cdot f(N_{\text{cs},m}) + X_{jm}\gamma + \xi_{jm}, \quad (16)$$

where s_{jm} is the observed market share of product j defined in Equation 25 and s_{0m} is the outside-good share. Standard errors are clustered at the market level.

4.2 Identification Strategy

Estimation of equation (16) faces two endogeneity concerns: price p_{jm} is correlated with unobserved characteristics ξ_{jm}, and infrastructure counts $N_{\text{gs},m}$ and $N_{\text{cs},m}$ may respond to local demand conditions. Unobserved characteristics may simultaneously influence firms' pricing decisions, and infrastructure investment. For example, a positive demand shock for EVs in a given market could lead to both higher prices and greater charging station deployment, creating simultaneity bias.

For vehicle prices, we follow Barwick et al. (2024) and employ three sets of instrumental variables: (1) central government purchase subsidies, (2) vehicle purchase tax rates, and (3) measures of product differentiation within market segments. Central subsidies directly affect transaction prices and follow discrete schedules based on vehicle attributes such as driving range. These policy-induced discontinuities generate exogenous variation in prices that is unlikely to be correlated with unobserved demand shocks. Purchase tax rates similarly shift prices through policy variation that is determined independently of product-level demand conditions. The third set of instruments captures within-segment product differentiation. Let x_{kj} denote characteristic k of product j, where x_j is the vector of observed product characteristics, including log size, engine displacement, electric efficiency, fuel efficiency, and log driving range. For each product j, we construct instruments based on the set of products within the same market segment s, where a segment is defined by the combination of product j's body type (e.g., sedan, SUV), fuel type (e.g., EV or ICE), and market m. Let n_s denote the number of products in segment s. For each characteristic k, we compute the leave-one-out mean among other products in the same segment and construct a differentiation instrument as the absolute deviation from this segment mean. These instruments capture the extent of within-segment product differentiation, which affects equilibrium pricing through competitive interactions but is unlikely to be correlated with unobserved demand shocks, conditional on controls and fixed effects.

To address the endogeneity of charging infrastructure, we construct Bartik-style shift-share instruments following Li et al. (2017). Specifically, for EV charging stations, we interact the number of grocery stores and supermarkets in a city in 2014 (pre-sample) with two aggregate time-varying components. First, we interact it with the lagged number of charging stations in all other cities, which captures national trends in charging station deployment driven by aggregate shocks such as changes in costs, investor expectations, and

policy support. Second, we interact it with the lagged national construction cost of charging stations, which reflects time variation in investment costs. Grocery stores and supermarkets are major hosts of charging stations, as they install them to attract customers and enhance green credentials. The exclusion restriction for infrastructure instruments relies on the fact that 2014 POI density reflects pre-existing urban geography rather than contemporaneous vehicle demand shocks, conditional on city fixed effects. The pre-sample distribution of these locations provides cross-sectional variation in the suitability of markets for charging infrastructure. While this variation is time-invariant and absorbed by fixed effects, interacting it with national time-varying factors generates exogenous variation in local charging station deployment. This strategy isolates supply driven changes in infrastructure that are plausibly orthogonal to local unobserved demand shocks.

For gas stations, we construct analogous instruments using transportation-related POIs in each city in 2014 (pre-sample), including highway service areas, auto repair shops, bus terminals, car wash services, and auto parts retailers. We interact these measures with two aggregate time-varying components. First, we interact them with the lagged number of gas stations in all other cities, which captures national trends in gas station deployment driven by aggregate shocks such as changes in fuel demand, investment conditions, and industry expansion. Second, we interact them with the lagged national average oil price, which reflects time variation in operating profitability and incentives for gas station investment. These POIs proxy for the local suitability and pre-existing infrastructure for gas station placement. While their cross-sectional variation is time-invariant and absorbed by fixed effects, interacting them with national trends generates exogenous variation in local gas station supply that is plausibly orthogonal to local demand shocks.

We estimate the demand model in two stages under alternative specifications for infrastructure. In the baseline, infrastructure enters as $f(N) = \log(N)$, and we estimate equation (16) using two-stage least squares (2SLS). The first stage regresses $\log p_{jm}$ on the full set of instruments and exogenous controls, and the second stage regresses $\log(s_j/s_0)$ on the predicted price and infrastructure measures. Table 2 reports the results. Infrastructure enters utility through a flexible transformation $f(\cdot)$ interacted with fuel-type indicators, allowing ICE vehicles to benefit from gas station availability and EVs from charging infrastructure. This captures indirect network effects: denser infrastructure raises the utility of the corresponding vehicle type and promotes adoption. To allow for flexible curvature,

we generalize the specification to a CRRA (constant relative risk aversion) functional form:

$$f(N;\gamma) = \frac{N^{1-\gamma} - 1}{1-\gamma}, \tag{17}$$

which nests the logarithmic case as $\gamma \to 1$ and the linear case as $\gamma = 0$. We estimate separate curvature parameters for charging stations and gas stations, allowing for different degrees of diminishing returns. Because γ enters nonlinearly, we adopt a concentrated nonlinear least squares (NLS) approach: we first instrument price and infrastructure using the IVs described above, then estimate the remaining parameters conditional on γ, and select the optimal values by minimizing the sum of squared residuals.

4.3 Estimation Results

Table 2 reports demand estimates across five specifications that vary in estimator, instrument strategy, and the functional form of infrastructure. Columns (1)–(2) estimate linear specifications in which infrastructure enters as $\log(N)$, with column (1) using OLS and column (2) instrumenting price. Column (3) estimates a nonlinear specification in which infrastructure enters through a CRRA transformation, while column (4) extends the linear specification by instrumenting both price and infrastructure. Column (5) reports the corresponding GMM estimates using the full set of instruments and optimal weighting.

When the potential endogeneity of price and driving range is not addressed, the estimated price coefficient is small in magnitude, as in the OLS logit specification. Favorable demand shocks induce firms to set higher prices, generating a positive correlation between price and unobserved demand that biases the OLS estimate toward zero. Instrumenting for price substantially increases the magnitude of the coefficient, from -0.32 in OLS to approximately -3.7 to -4.3 in the IV and GMM specifications, indicating severe attenuation bias. The GMM estimates are larger in magnitude than the corresponding 2SLS estimates, consistent with the use of an efficient weighting matrix in an overidentified system.

Infrastructure coefficients are positive and precisely estimated across all specifications, providing strong evidence of indirect network effects. In the linear specifications, the charging station effect for EVs ranges from 0.323 to 0.465, while the gas station effect for ICE vehicles ranges from 0.313 to 0.411. Estimates from the nonlinear specifications are smaller in levels but remain precisely estimated. The GMM results imply larger marginal

Table 2: Demand Estimates

	(1) OLS	(2) Price IV	(3) NLS	(4) Full IV	(5) GMM
Vehicle characteristics					
log(Price)	-0.320^{***}	-3.779^{***}	-3.803^{***}	-3.689^{***}	-4.513^{***}
	(0.024)	(0.107)	(0.066)	(0.113)	(0.105)
$\mathbf{1}_{\text{EV}} \times$ log(Range)	0.713^{***}	0.548^{***}	0.384^{***}	0.327^{***}	0.540^{***}
	(0.057)	(0.089)	(0.048)	(0.095)	(0.062)
log(Volume)	4.347^{***}	8.748^{***}	8.735^{***}	8.655^{***}	9.594^{***}
	(0.074)	(0.135)	(0.097)	(0.139)	(0.149)
log(Power)	0.331^{***}	2.219^{***}	2.234^{***}	2.164^{***}	2.674^{***}
	(0.025)	(0.069)	(0.042)	(0.070)	(0.063)
$\mathbf{1}_{\text{EV}} \times$ Elec. consumption	-0.016^{*}	-0.025^{*}	-0.025^{***}	-0.019	-0.008
	(0.009)	(0.013)	(0.010)	(0.011)	(0.009)
$\mathbf{1}_{\text{ICE}} \times$ Fuel consumption	-0.638^{***}	-0.400^{***}	-0.392^{***}	-0.408^{***}	-0.346^{***}
	(0.008)	(0.012)	(0.007)	(0.013)	(0.009)
Infrastructure parameters					
$\mathbf{1}_{\text{EV}} \times f(N_{\text{cs}})$	0.401^{***}	0.323^{***}	0.186^{***}	0.465^{***}	0.323^{***}
	(0.014)	(0.015)	(0.004)	(0.030)	(0.010)
$\mathbf{1}_{\text{ICE}} \times f(N_{\text{gs}})$	0.339^{***}	0.313^{***}	0.144^{***}	0.411^{***}	0.223^{***}
	(0.015)	(0.016)	(0.003)	(0.025)	(0.006)
γ_{cs}			0.898		0.899
			(.)		(.)
γ_{gs}			0.880		0.881
			(.)		(.)
$f(\cdot)$ form	$\log(N+1)$	$\log(N+1)$	CRRA	$\log(N+1)$	CRRA
IV for price	No	Yes	Yes	Yes	Yes
IV for CS, GS	No	No	No	Yes	Yes
N	496,806	496,806	496,806	496,806	496,806

Notes: $^{***}p < 0.01$, $^{**}p < 0.05$, $^{*}p < 0.1$.
All specifications absorb brand, year, city, fuel type, body type, and duration fixed effects, with standard errors clustered at the market (city-year) level. Column (1) reports OLS. Column (2) instruments price only, while charging and gas station availability enter directly as exogenous controls in log form. Column (3) estimates a nonlinear demand specification in which infrastructure enters through a CRRA transformation, with separate curvature parameters for charging and gas stations; price is instrumented. Column (4) estimates a linear 2SLS specification instrumenting price, charging stations, and gas stations. Column (5) reports the corresponding GMM estimates using the full set of instruments. In columns (1), (2), and (4), infrastructure enters as $\log(N)$. In columns (3) and (5), infrastructure enters through the CRRA form $h(N;\gamma) = \left(N^{1-\gamma}-1\right)/(1-\gamma)$.

effects, reflecting both the nonlinear functional form and additional moment conditions.

The similarity in magnitude between charging and gas infrastructure coefficients indicates broadly symmetric network effects across the two technologies.

The CRRA specifications in columns (3) and (5) allow for flexible curvature in the relationship between infrastructure and demand. The estimated curvature parameters, in the NLS specification, imply diminishing marginal returns to infrastructure expansion. The GMM estimates yield slightly higher curvature, particularly for charging stations, but remain within a comparable range. Overall, the results support a concave relationship between infrastructure density and demand.

Vehicle characteristics enter with expected signs and are stable across specifications. Larger vehicles and higher power increase demand, while higher energy consumption reduces demand. Driving range for EVs has a positive and statistically significant effect, highlighting the importance of technological attributes in adoption decisions. In contrast, EV electricity consumption is not statistically significant in some specifications, suggesting that EV consumers place limited weight on operating costs, consistent with low electricity prices and the prevalence of free or subsidized charging services.

Taken together, the results provide robust evidence of positive indirect network effects operating through refueling infrastructure. The comparable magnitudes of charging and gas station effects suggest that both sides of the dual network operate with similar strength. At the same time, the concavity implied by both log and CRRA specifications indicates diminishing marginal effects, implying that infrastructure expansion alone is unlikely to generate sharp tipping behavior absent additional nonlinear mechanisms.

5 Charging Station Entry Model

5.1 Descriptive Evidence: State-Dependent Network Effects

Before turning to the structural entry model, we present reduced-form evidence that both the supply-side and demand-side network effects vary with EV market maturity. This motivates the S-shaped entry model and provides a model-free check on the nonlinearity that is central to the tipping mechanism.

Supply: CS entry elasticity by adoption bin. We partition the city-year panel into five bins of EV stock share (s_{ev}) and estimate, within each bin, the pooled OLS elasticity of CS density with respect to EV stock: $\partial \log d_{\text{cs}} / \partial \log S_{\text{ev}}$. Panel A of Figure 9 shows that the supply-side entry elasticity is positive and statistically significant in all bins, ranging from 0.27 to 0.64. While the point estimates are imprecise in some bins due to small sample sizes, the overall pattern is consistent with a supply response that is active at all stages of adoption rather than concentrated in a single phase.

Demand: β_{cs} by adoption bin. We interact the Bartik-instrumented CS measure with bin indicators in the IV-logit demand equation, allowing the charging infrastructure coefficient β_{cs} to vary across adoption stages. Panel B of Figure 9 reveals a monotonic pattern. This pattern implies that the demand-side network effect is effectively inactive — or even negative — when the EV market is nascent, but becomes a strong positive force once adoption exceeds a critical mass.

Implications. The demand-side pattern is consistent with a threshold mechanism: at very low EV shares, adding charging stations does not attract EV buyers (perhaps because the technology is still unfamiliar or the stations are poorly utilized), but once a minimum network is in place, each additional station meaningfully reduces range anxiety and boosts demand. This nonlinearity is precisely what generates tipping dynamics in the structural model: the feedback loop between CS supply and EV demand strengthens with adoption, creating the possibility of multiple equilibria.

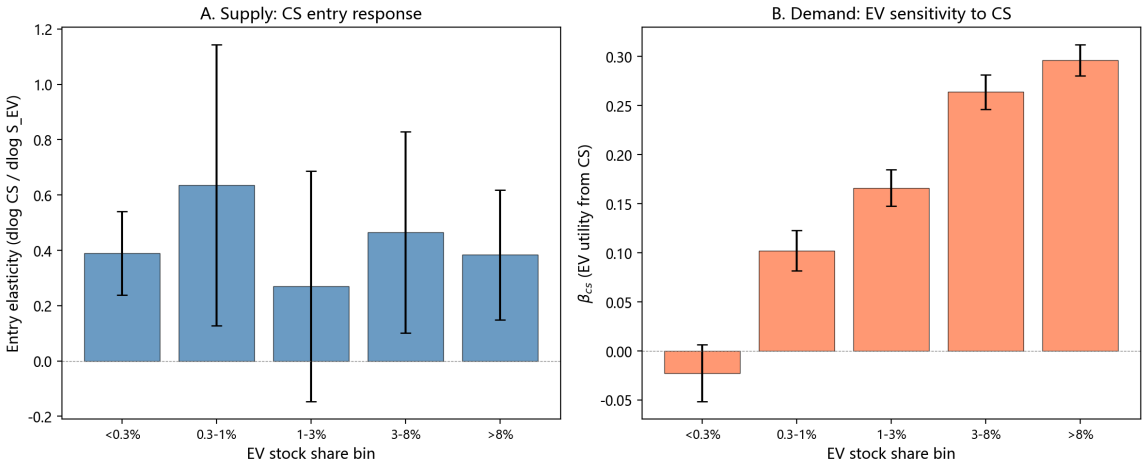

Figure 9: Descriptive evidence of state-dependent network effects. Panel A: Supply-side CS entry elasticity ($\partial \log d_{\text{cs}} / \partial \log S_{\text{ev}}$) estimated by pooled OLS within each EV stock share bin. Panel B: Demand-side charging infrastructure coefficient $\hat{\beta}_{\text{cs}}$ estimated via IV-logit with bin-specific interactions (Bartik IV for CS, Diff IV for price). Error bars show 95% confidence intervals with HC1 standard errors. The demand-side coefficient transitions from significantly negative at low EV shares to significantly positive at high shares, providing model-free evidence of the nonlinear feedback that underlies tipping.

5.2 Dynamic Entry Model

We model charging station entry as a dynamic discrete-choice problem (Aguirregabiria and Mira, 2007). Section 5.2 sets up the entry framework and derives the micro-founded profit function. Section 5.3 specifies how consumer adoption responds to the resulting infrastructure.

Each potential charging station location ℓ in tier $\tau \in \{\text{commercial, thriving, remote}\}$ of city c at time t faces an irreversible entry decision. The operator pays a one-time sunk cost $F_{\tau c}$ upon entry and receives a per-period flow profit $\Pi_{\tau ct}$ that depends on the local EV stock share and the density of competing stations.

Micro-foundation of the flow profit. We derive the functional form of $\Pi_{\tau ct}$ from a standard CES demand framework.

Proposition 1 (CES Profit Function)**.** *Suppose EV owners have CES preferences over charging stations with elasticity of substitution $\varepsilon > 1$. Let s denote the EV stock share, N_{cs} the number of charging stations, and c^e the marginal cost of electricity. Then the oper-*

ating profit of station i in market m is:

$$\Pi^*_{im} = A_{im} \cdot \frac{s^{\gamma^{EV}}}{N^{\gamma^{CS}}_{cs}} \cdot B(\varepsilon) \cdot (c^e)^{1-\varepsilon}, \tag{18}$$

where γ^{EV} and γ^{CS} are endogenously determined by the CES structure, A_{im} captures station-level heterogeneity in quality and location, and $B(\varepsilon) = (\varepsilon-1)^{\varepsilon-1}/\varepsilon^{\varepsilon}$ is a markup constant.

Proof. Under CES demand, the quantity demanded at station i is $q_i = s \cdot (p_i/P)^{-\varepsilon}$, where $P = \left(\sum_{j=1}^{N_{cs}} p_j^{1-\varepsilon}\right)^{1/(1-\varepsilon)}$ is the aggregate price index. With symmetric marginal costs c^e, all stations set the markup price $p^* = \frac{\varepsilon}{\varepsilon-1} c^e$, giving $P = N_{cs}^{1/(1-\varepsilon)} p^*$, $q^* = s/N_{cs}$, and $\Pi^* = (p^* - c^e)\, q^*$. Substitution yields the result with $\gamma^{EV} = 1$ and $\gamma^{CS} = 1$ in the symmetric case. Heterogeneity in station quality or spatial differentiation allows these elasticities to deviate from unity in estimation. ∎

Applying Proposition 1, the flow profit at location ℓ of tier τ in city c is:

$$\Pi_{\tau ct} = \tilde{\theta}(\tau, c) \cdot \frac{s_{ct}^{\gamma^{EV}}}{N^{\gamma^{CS}}_{cs,ct}} \cdot B(\varepsilon) + \theta_{\text{sub},u} \cdot \text{SubsidyUsage}_{ct}, \tag{19}$$

where the profit coefficient $\tilde{\theta}$ varies by tier and city characteristics:

$$\tilde{\theta}(\tau, c) = \theta_0 + \theta_\tau + \delta' X_c, \tag{20}$$

with θ_τ capturing tier-specific profit shifts (commercial $= 0$ as base) and X_c a vector of standardized city characteristics (log GDP per capita, log population density, urbanization rate, log area per hex). The sunk cost similarly varies:

$$F_{\tau c} = F_0 + F_\tau + \phi' X_c - \theta_{\text{sub},c} \cdot \text{SubsidyConstr}_{ct}. \tag{21}$$

Oblivious equilibrium and the entry decision. Each station operator takes the aggregate state as given and expects the EV stock and charging station density to grow at constant rates g^{EV} and g^{CS} (Weintraub et al., 2008). Under this **oblivious equilibrium**, the present

value of entering at the current state is:

$$W_{\tau ct} = \frac{\Pi_{\tau ct}}{1-\tilde{\beta}}, \qquad \tilde{\beta} = \beta \cdot \frac{(1+g^{EV})^{\gamma^{EV}}}{(1+g^{CS})^{\gamma^{CS}}}, \tag{22}$$

where β is the annual discount factor. Each location draws an idiosyncratic cost shock $\varepsilon_{\ell t} \sim$ Type-I EV$(0,1)$. Location ℓ enters if $W_{\tau ct} - F_{\tau c} > \varepsilon_{\ell t}$, giving the conditional choice probability (CCP):

$$p_{\tau ct} = \Lambda\big(W_{\tau ct} - F_{\tau c}\big), \tag{23}$$

where $\Lambda(\cdot)$ is the logistic CDF. The equilibrium number of new charging stations of tier τ is $N^{\text{new}}_{cs,\tau ct} = L_{\tau c} \cdot p_{\tau ct}$, where $L_{\tau c}$ is the number of potential entry locations.

5.3 Consumer Adoption

Charging station entry feeds back to consumer adoption through a network effect. We model the EV purchase share among new cars as a logit function of the infrastructure state:

$$\pi^{ev}_{ct} = \frac{\exp\big(\xi^{EV}_{ct} + \alpha \ln(N_{cs,ct})\big)}{\exp\big(\xi^{EV}_{ct} + \alpha \ln(N_{cs,ct})\big) + \exp\big(\xi^{GV}_{ct} + \alpha \ln N_{gs,ct}\big)}, \tag{24}$$

where $\alpha > 0$ is the network elasticity, ξ^{EV}_{ct} and ξ^{GV}_{ct} are composite indices of vehicle quality and policy (subsuming prices, product attributes, and purchase subsidies), and $N_{gs,ct}$ is the gas station count. The key feedback loop is: a higher EV share s raises station profitability (19), inducing entry, which raises N_{cs}, which raises π^{ev}, which in turn increases s in the next period.

6 Estimation

We propose estimating the structural parameters using a two-stage CCP approach (Aguirregabiria and Mira, 2007), which avoids the computational cost of full-solution dynamic programming.

First stage: CCPs and state transitions. We estimate the flow entry probabilities $\hat{p}_{\tau ct}$ from the data using smoothed CCPs. The observed state variables — EV share s_{ct}, station

counts $N_{cs,ct}$, subsidies, and city characteristics — are taken directly from the data.

Second stage: structural parameters. The CES parameters $(\varepsilon, \gamma^{EV}, \gamma^{CS})$ enter the profit function nonlinearly, while the remaining parameters — profit coefficients $(\theta_0, \theta_\tau, \delta)$, subsidy effects (θ_{sub}), and sunk costs (F_0, F_τ, ϕ) — enter linearly conditional on the CES parameters. We adopt a **concentrated NLS** approach: for each candidate $(\varepsilon, \gamma^{EV}, \gamma^{CS})$ on a grid, we compute the CES profit index $\tilde{x}_{ct} \equiv s_{ct}^{\gamma^{EV}} / N_{cs,ct}^{\gamma^{CS}} \cdot B(\varepsilon)$ and recover the linear parameters by OLS regression of the log-odds of entry on the profit index (interacted with tier and city characteristics), subsidies, and sunk cost shifters. We select the $(\varepsilon, \gamma^{EV}, \gamma^{CS})$ that minimize the sum of squared residuals. Standard errors are clustered at the city level.

Refinement. The two-step estimates can be refined via the Nested Pseudo-Likelihood (NPL) algorithm (Aguirregabiria and Mira, 2007), which iterates between updating the CCPs using the estimated structural parameters and re-estimating the parameters using the updated CCPs, until convergence.

7 Illustrative Simulation

To illustrate the equilibrium structure implied by the model, we simulate the long-run steady state under a benchmark calibration and evaluate how policy interventions can eliminate the low-adoption trap.

7.1 Setup

We set the CES parameters to $\varepsilon = 2.5$, $\gamma^{EV} = 1.2$, $\gamma^{CS} = 0.8$, with discount factor $\beta = 0.80$ and growth rates $g^{EV} = 0.15$, $g^{CS} = 0.05$, yielding an effective discount factor $\tilde{\beta} \approx 0.91$. Station quality A_i and entry costs F_i are drawn from lognormal distributions to generate firm heterogeneity. To model the outside option, gas stations exit in two stages: short-lease stations ($N_{\text{short}} = 20$) exit around $s = 0.20$, while long-lease stations ($N_{\text{long}} = 35$) persist until $s \approx 0.55$.

For each EV share $s \in [0, 1]$, we solve for the free-entry equilibrium $N_{cs}^*(s)$ — the station count at which the sum of individual entry probabilities equals the aggregate number of entrants. We apply a market-development factor $\delta(s) = 1 - e^{-s/0.01}$ to ensure $N_{cs}^*(0) = 0$.

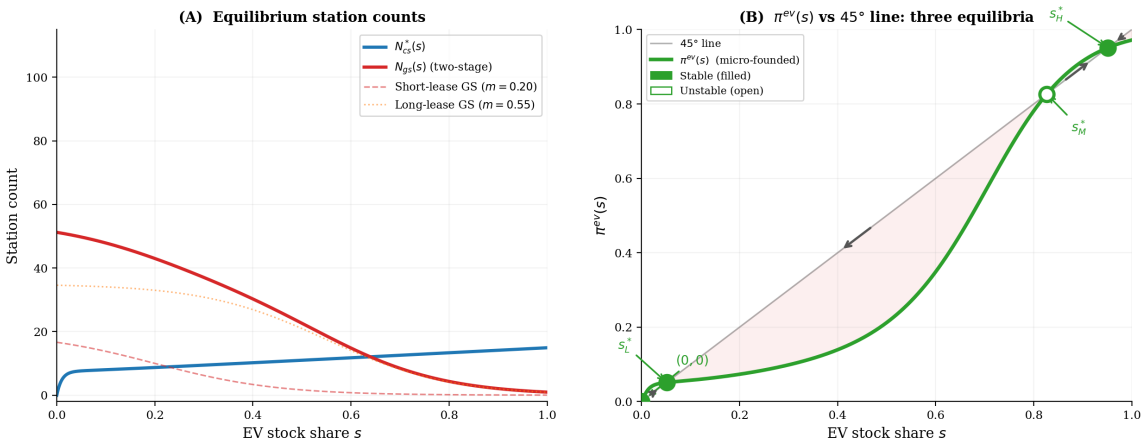

Figure 10: Benchmark simulation. Panel (A): equilibrium station counts. Panel (B): $\pi^{ev}(s)$ versus the 45-degree line. Filled circles = stable; open circles = unstable.

The consumer adoption mapping $\pi^{ev}(s)$ then follows from (24), and a steady state requires $\pi^{ev}(s^*) = s^*$.

7.2 Benchmark Equilibria

Figure 10 presents the results. Panel (A) shows $N^*_{cs}(s)$ rising smoothly from zero while $N_{gs}(s)$ declines in two stages. Panel (B) plots $\pi^{ev}(s)$ against the 45-degree line, revealing four equilibria:

- $(0,0)$: the corner equilibrium — no EVs, no stations.
- $s^*_L \approx 0.05$: a **stable low-adoption trap**, sustained by the large stock of gas stations.
- $s^*_M \approx 0.83$: the **unstable tipping point**. Below it, the system reverts to s^*_L; above it, the network effect becomes self-reinforcing.
- $s^*_H \approx 0.95$: the **stable high-adoption** steady state.

7.3 Policy Counterfactuals

We evaluate three policy levers: (i) a **construction subsidy** τ^{cnst} that reduces the sunk cost F_i; (ii) a **usage subsidy** τ^{usage} that scales up flow profitability via $(1-\tau^{usage})^{1-\varepsilon}$; and (iii) **GS exit acceleration** τ^{gs} that shifts gas station exit midpoints leftward.

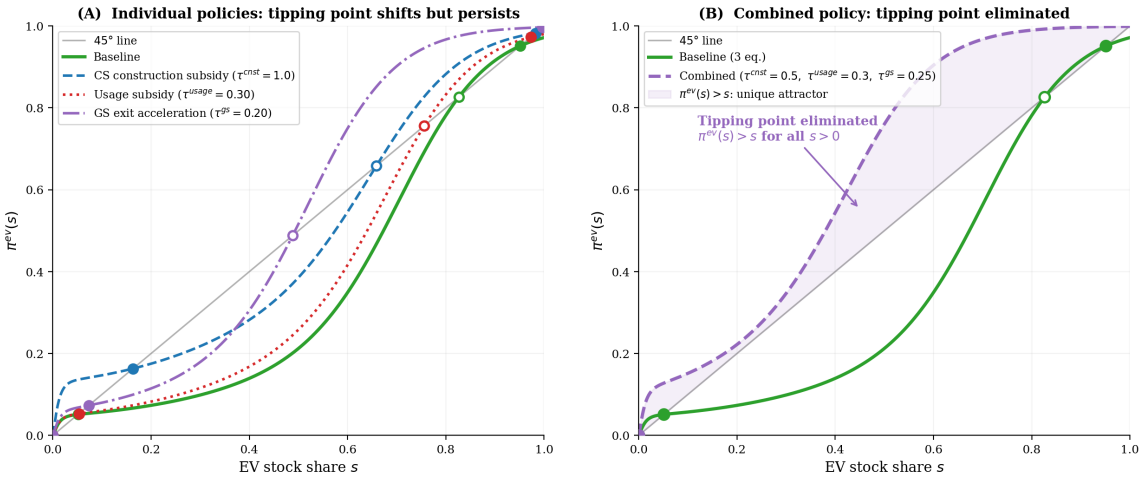

Figure 11: Policy counterfactuals. Panel (A): individual policies preserve the S-shape. Panel (B): combined policy places $\pi^{ev}(s)$ entirely above the 45-degree line.

Figure 11 shows that each individual policy shifts $\pi^{ev}(s)$ upward and moves the tipping point leftward, but the multi-equilibrium structure persists (Panel A). A **combined policy** ($\tau^{cnst} = 0.5$, $\tau^{usage} = 0.30$, $\tau^{gs} = 0.25$) eliminates the tipping point entirely: $\pi^{ev}(s) > s$ for all $s > 0$, making the high-adoption state the unique attractor (Panel B). The three channels are complementary: construction subsidies increase station density, usage subsidies amplify flow profits, and GS exit acceleration weakens the outside option. No single instrument is sufficient because each addresses only one of the three barriers — sunk cost, flow profit, and the outside option — that jointly sustain the coordination failure.

References

Acemoglu, Daron, Philippe Aghion, Leonardo Bursztyn, and David Hemous, "The Environment and Directed Technical Change," *American Economic Review*, 2012, *102* (1), 131–166.

_ **, Ufuk Akcigit, Douglas Hanley, and William Kerr**, "Transition to Clean Technology," *Journal of Political Economy*, 2016, *124* (1), 52–104.

Ackerberg, Daniel A. and Gautam Gowrisankaran, "Quantifying Equilibrium Network Externalities in the ACH Banking Industry," *RAND Journal of Economics*, 2006, *37* (3).

Aghion, Philippe, Antoine Dechezleprêtre, David Hémous, Ralf Martin, and John Van Reenen, "Carbon Taxes, Path Dependency, and Directed Technical Change: Evidence from the Auto Industry," *Journal of Political Economy*, 2016, *124* (1), 1–51.

_ , Lint Barrage, Eric Donald, David Hémous, and Ernest Liu, "Transition to Green Technology along the Supply Chain," 2025. NBER Working Paper 33934.

Aguirregabiria, Victor and Pedro Mira, "Sequential Estimation of Dynamic Discrete Games," *Econometrica*, 2007, *75* (1), 1–53.

Armstrong, Mark, "Competition in Two-Sided Markets," *RAND Journal of Economics*, 2006, *37* (3).

Bartik, Timothy J., "Who Benefits from State and Local Economic Development Policies?," 1991.

Barwick, Panle J., Hyuk-soo Kwon, and Shanjun Li, "Attribute-Based Subsidies and Market Power: An Application to Electric Vehicles," 2024. NBER Working Paper 32264.

_ , _ , _ , and Nahim B. Zahur, "Drive Down the Cost: Learning by Doing and Government Policies in the Global EV Battery Industry," 2025. NBER Working Paper 33378.

Barwick, Panle Jia, Shanjun Li, and Tianli Xia, "Range Anxiety," 2026. NBER Working Paper 34871.

Berry, Steven, James Levinsohn, and Ariel Pakes, "Automobile Prices in Market Equilibrium," *Econometrica*, 1995, *63* (4), 841–890.

Björkegren, Daniel, "The Adoption of Network Goods: Evidence from the Spread of Mobile Phones in Rwanda," *Review of Economic Studies*, 2019, *86* (3).

_ , "Competition in Network Industries: Evidence from the Rwandan Mobile Network," *RAND Journal of Economics*, 2022, *53* (2).

Bollinger, Bryan, Naim Darghouth, Kenneth Gillingham, and Andres Gonzalez-Lira, "Valuing technology complementarities: Rooftop solar and energy storage," 2024. NBER Working Paper.

Brown, Jennifer and John Morgan, "How Much Is a Dollar Worth? Tipping versus Equilibrium Coexistence on Competing Online Auction Sites," *Journal of Political Economy*, 2009, *117* (4).

Butters, R. Andrew, Jackson Dorsey, and Gautam Gowrisankaran, "Soaking up the Sun: Battery Investment, Renewable Energy, and Market Equilibrium," *Econometrica*, 2025, *93* (3), 891–927.

Cao, Guangyu, Ginger Zhe Jin, Xi Weng, and Li-An Zhou, "Market-Expanding or Market-Stealing? Competition with Network Effects in Bike-Sharing," *RAND Journal of Economics*, 2021, *52* (2).

Dorsey, Jackson, "Solar Market Frictions: The Role of Platforms and Policies," *The Review of Economics and Statistics*, 2024, pp. 1–45.

Dugoua, Eugenie and Jacob Moscona, "The Economics of Climate Innovation: Technology, Climate Policy, and the Clean Energy Transition," 2025. NBER Working Paper 34601.

Ellison, Glenn, Drew Fudenberg, and Markus M. Möbius, "Knife-Edge or Plateau: When Do Market Models Tip?," *Quarterly Journal of Economics*, 2003, *118* (3).

Ericson, Richard and Ariel Pakes, "Markov-Perfect Industry Dynamics: A Framework for Empirical Work," *The Review of Economic Studies*, 1995, *62* (1), 53–82.

Fang, Hanming, Ming Li, Long Wang, and Yang Yang, "High-Speed Rail and Electric Vehicle Adoption," 2025. NBER Working Paper 33489.

Farrell, Joseph and Garth Saloner, "Installed Base and Compatibility: Innovation, Product Preannouncements, and Predation," *American Economic Review*, 1986, *76* (5).

Feger, Fabian, Nicola Pavanini, and Doina Radulescu, "Welfare and Redistribution in Residential Electricity Markets with Solar Power," *The Review of Economic Studies*, 2022, *89* (6), 3267–3302.

Gandal, Neil, "Hedonic Price Indexes for Spreadsheets and an Empirical Test for Network Externalities," *RAND Journal of Economics*, 1994, *25* (1).

_ , "Competing Compatibility Standards and Network Externalities in the PC Software Market," *Review of Economics and Statistics*, 1995, *77* (4).

Garcia-Osipenko, Maria, "Technology Complementarities and Subsidy Policy: Evidence from Electric Vehicle and Solar Panel Adoption," *Available at SSRN 4815511*, 2025.

Goldsmith-Pinkham, Paul, Isaac Sorkin, and Henry Swift, "Bartik Instruments: What, When, Why, and How," *American Economic Review*, 2020, *110* (8), 2586–2624.

Groote, Olivier De and Frank Verboven, "Subsidies and Time Discounting in New Technology Adoption: Evidence from Solar Photovoltaic Systems," *American Economic Review*, 2019, *109* (6), 2137–2172.

Holland, Stephen P., Erin T. Mansur, and Andrew J. Yates, "The Electric Vehicle Transition and the Economics of Banning Gasoline Vehicles," *American Economic Journal: Economic Policy*, 2021, *13* (3), 316–344.

Hotz, V. Joseph and Robert A. Miller, "Conditional Choice Probabilities and the Estimation of Dynamic Models," *The Review of Economic Studies*, 1993, *60* (3), 497–529.

Hu, Yunyi, Haitao Yin, and Li Zhao, "Subsidy Phase-Out and Consumer Demand Dynamics: Evidence from the Battery Electric Vehicle Market in China," *The Review of Economics and Statistics*, 2025, *107* (2), 458–475.

Katz, Michael L. and Carl Shapiro, "Network Externalities, Competition, and Compatibility," *American Economic Review*, 1985, *75* (3), 424–440.

_ **and** _ , "Technology Adoption in the Presence of Network Externalities," *Journal of Political Economy*, 1986, *94* (4).

Kwon, Hyuk-soo, "Subsidies versus tradable credits for electric vehicles: The role of market power in the credit market," *Available at SSRN 5160795*, 2026.

Li, Jing, "Compatibility and Investment in the U.S. Electric Vehicle Market," 2023. Latest public version (2023), R&R (second round), American Economic Review.

Li, Shanjun, Lang Tong, Jianwei Xing, and Yiyi Zhou, "The Market for Electric Vehicles: Indirect Network Effects and Policy Design," *Journal of the Association of Environmental and Resource Economists*, 2017, *4* (1), 89–133.

Lohawala, Nafisa, "Roadblock or accelerator? The effect of electric vehicle subsidy elimination," *Resources for the Future Working Paper*, 2023, pp. 23–13.

Meunier, Guy and Jean-Pierre Ponssard, "Optimal policy and network effects for the deployment of zero emission vehicles," *European Economic Review*, 2020, *126*, 103449.

Remmy, Kevin, "Adjustable Product Attributes, Indirect Network Effects, and Subsidy Design: The Case of Electric Vehicles," *American Economic Journal: Economic Policy*, 2025. Forthcoming.

Rochet, Jean-Charles and Jean Tirole, "Platform Competition in Two-Sided Markets," *Journal of the European Economic Association*, 2003, *1* (4).

Rust, John, "Optimal Replacement of GMC Bus Engines: An Empirical Model of Harold Zurcher," *Econometrica*, 1987, *55* (5), 999–1033.

Springel, Katalin, "Network Externality and Subsidy Structure in Two-Sided Markets: Evidence from Electric Vehicle Incentives," *American Economic Journal: Economic Policy*, 2021, *13* (4), 476–510.

Weintraub, Gabriel Y., C. Lanier Benkard, and Benjamin Van Roy, "Markov perfect industry dynamics with many firms," *Econometrica*, 2008, *76* (6), 1375–1411.

A Subsidy Policy Construction Details

This appendix provides detailed information on the construction of the EV purchase subsidy and charging station subsidy variables described in Section 3.1.

A.1 Central EV Purchase Subsidies

The central subsidy schedules were jointly formulated and promulgated by four governmental bodies: the Ministry of Industry and Information Technology (MIIT), the Ministry of Finance (MoF), the Ministry of Science and Technology (MoST), and the National Development and Reform Commission (NDRC). We coded the subsidy calculation rules for each year based on the official policy documents published by MIIT.

The eligibility thresholds were progressively tightened over the sample period. The minimum electric range for BEV subsidies rose from 80 km in 2013 to 100 km in 2016 and further to 150 km in 2018. A minimum battery system energy density requirement was introduced starting in 2017. Moreover, from 2018 onward, subsidy amounts were no longer determined solely by driving range but were simultaneously adjusted by a battery energy density coefficient and an energy consumption efficiency coefficient. This dual mechanism of declining subsidies and rising technical thresholds steered the industry toward longer range, higher energy density, and greater energy efficiency.

We combined these coded rules with vehicle-specific technical parameters from the sales data—including electric driving range, battery energy density, energy consumption per 100 km, and battery capacity—to compute the central subsidy amount for each vehicle model in each year.

A.2 Local EV Purchase Subsidies

The design of local subsidies exhibits substantial cross-city heterogeneity along several dimensions. Most cities adopted a ratio-based approach, setting local subsidies as a proportion of the central subsidy—typically ranging from 20% to 100%—while imposing a cap on the total subsidy (central plus local) as a share of vehicle price. Some cities in certain years instead adopted a fixed-amount approach, specifying subsidy amounts directly based on tiered electric driving range cutoffs. Local subsidies also varied by fuel type (with BEVs generally receiving higher subsidies than PHEVs) and vehicle body size.

Using data from the PKULAW legal database, we systematically compiled local subsidy policies across sample markets for the period 2016–2019, coded the subsidy rules for each city across different time periods and vehicle types, and combined these with vehicle parameters to compute the local subsidy amount for each vehicle model.

A.3 Charging Station Subsidies: Magnitudes in Perspective

To put the charging station subsidy figures in perspective, consider a typical public DC fast-charging station with a rated capacity of roughly 400 kW (e.g., 8 guns $\times$ 60 kW). At the peak national construction subsidy of 600 RMB/kW (2015–2016), such a station received a one-time grant of approximately 240,000 RMB, covering an estimated 20–40% of total installation costs. By 2023, the average effective construction subsidy across our 34 sample cities had fallen to roughly 150 RMB/kW, translating to about 63,000 RMB per station—less than 10% of installation costs.

On the operating side, usage subsidies averaged 0.56 RMB/kWh across city-years with positive subsidies (declining from $\sim$0.65 in 2016–2018 to $\sim$0.35 by 2023–2024). At a representative utilization of 500 kWh/day, this yields annual operating-subsidy revenue of 60,000–120,000 RMB per station. In sum, early entrants benefited from substantial construction grants and steady usage subsidies, while later entrants faced a much thinner subsidy envelope.

B Market Definition

We define each location c as either a city or a provincial residual market. we construct 52 target cities, comprising all 19 tier-1 and new-tier-1 cities and 33 key tier-2 cities selected on the basis of population and economic significance. Vehicle registrations in districts outside these 52 cities are aggregated into provincial residual markets, so that the union of target cities and residual markets covers all new passenger vehicle registrations nationwide. A market m is defined as a location c paired with a year t.

We define market size as the number of households, $M_{ct} = \text{Population}_{ct}/(2.62 \times 10{,}000)$, where 2.62 is the average household size. The potential market is $M_{ct}/5$, reflecting an as-

sumed five-year vehicle replacement cycle. Product shares are given by

$$s_{jm} = \frac{Q_{jm}}{M_{ct}/5}, \tag{25}$$

where Q_{jm} is the quantity of product j sold in market m. The outside good share is defined as $s_{0m} = 1 - \sum_j s_{jm}$, representing households that do not purchase a new vehicle in year t.

We measure the transaction price as the MSRP, which includes the value-added tax, plus the vehicle purchase tax, and net of central and local purchase subsidies:

$$p_{jm} = \text{MSRP}_{jm} + \text{PurchaseTax}_{jm} - \text{CentralSubsidy}_{jm} - \text{LocalSubsidy}_{jm}. \tag{26}$$

Central government purchase subsidies for NEVs were phased out at the end of 2022, while local subsidies vary by city and year. All prices are expressed in units of 10,000 RMB. We drop observations with non-positive net prices.

C Data Details

This appendix provides additional details on the data construction described in Section 3.2.

C.1 Imputation of Missing Vehicle Characteristics

As described in Section 3.2, missing vehicle characteristics are imputed in two stages. First, we compute quantity-weighted means within brand-model-fuel type-year cells, with nearest-year interpolation to fill remaining gaps. Second, we apply multivariate imputation by chained equations (MICE) with Bayesian Ridge regression, implemented separately by fuel type group, to impute any characteristics still missing after the first stage.

C.2 Hex-Level Charging Station Data and Location Tiers

This subsection elaborates on the spatial data construction summarized in Section 3.2. We map charging station locations to H3 hexagonal grid cells at resolution 9 (approximately 0.105 km^2 per cell) and apply a one-year gap-filling and spike-removal procedure to correct likely reporting errors in the raw station data. Starting from 97.8 million hexagons covering mainland China, we retain 3.10 million hexagons classified as built-up (impervious surface)

in the CLCD 2019 land-cover data. We then classify each built-up hexagon into three tiers based on pre-sample (2014) POI density. For the current specification, we aggregate POI counts to the city level and use them to construct instruments for the endogenous variables. The 2014 POI data serve as a time-invariant geographic characteristic, determined prior to the EV adoption wave and thus free of simultaneity concerns.

C.3 Gas Station Data

City-year gas station counts are compiled from industry databases and matched to our market definition (Appendix B). We apply the same single-year gap-fill and spike-removal rule described above to correct reporting errors. These counts enter the tipping model via the calibrated exit equation.

Table 3: IV-Logit Demand Estimates: Mean IVs (Comparison)

	(A1)	(A2)	(A3)
Panel A: Price and Infrastructure			
$\log(\hat{p})$	6.416^{***}	5.565^{***}	5.957^{***}
	(0.209)	(0.228)	(0.224)
$\mathbf{1}_{\text{ICE}} \times f(N_{\text{gs}})$	0.354^{***}	0.298^{***}	0.301^{***}
	(0.007)	(0.008)	(0.008)
$\mathbf{1}_{\text{EV}} \times f(N_{\text{cs}})$	0.442^{***}	0.400^{***}	0.403^{***}
	(0.007)	(0.008)	(0.008)
Panel B: Vehicle Characteristics			
$\log(\text{Size})$	2.710^{***}	2.574^{***}	2.699^{***}
	(0.038)	(0.043)	(0.041)
Displacement	0.391^{***}	0.465^{***}	0.423^{***}
	(0.016)	(0.018)	(0.017)
$\mathbf{1}_{\text{EV}} \times \log(\text{Range})$	2.401^{***}	2.471^{***}	2.452^{***}
	(0.060)	(0.065)	(0.065)
$\mathbf{1}_{\text{EV}} \times \log(\text{Battery})$	-3.235^{***}	-3.244^{***}	-3.273^{***}
	(0.067)	(0.073)	(0.072)
Electric efficiency	-0.041^{***}	-0.038^{***}	-0.040^{***}
	(0.005)	(0.006)	(0.006)
Fuel efficiency	-0.601^{***}	-0.598^{***}	-0.603^{***}
	(0.005)	(0.006)	(0.005)
Macro controls	Yes	Yes	Yes
FE (brand, market, year, fuel, body)	Yes	Yes	Yes
Price IV	Mean	Mean	Mean
Infra. measure	$\log(N+1)$	Bartik	Bartik^{C}
R^2	0.371	0.373	0.372
N	490,700	392,219	421,972

Notes: Same specification as Table 2 columns (2)–(4), but using leave-one-out segment-mean IVs for price instead of Diff IVs. The positive price coefficients indicate that Mean IVs fail to resolve price endogeneity in this setting, motivating the use of Diff IVs as the preferred identification strategy.

D Additional Demand Estimation Results